QUARTERLY JOURNAL
OF THE
ROYAL METEOROLOGICAL SOCIETY

Vol. 112 JANUARY 1986 No. 471

Quart. J. R. Met. Soc. (1986), **112**, pp. 1–27 551.465.4:551.465.71

The response of the upper ocean to solar heating. I: The mixed layer

By J. D. WOODS and W. BARKMANN
Institut fuer Meereskunde an der Universitaet Kiel, F.R.G.

(Received 28 February 1985; revised 30 July 1985)

SUMMARY

The results of two earlier papers on convection in the mixed layer and on the solar heating profile are here introduced into a one-dimensional model in order to investigate the following consequences of the daily cycle of solar heating in the upper ocean:
1. the daytime convection depth becomes less than the turbocline depth;
2. the convective power supply to turbulence in the mixed layer is reduced;
3. the mixed layer below the convection layer becomes stably stratified;
4. the depth of the turbocline is reduced, leaving a diurnal thermocline between it and the top of the seasonal thermocline;
5. the heat content and potential energy of the diurnal and seasonal thermoclines are increased, slowing down the subsequent nocturnal descent of the turbocline.

These diurnal changes are illustrated by integrating a one-dimensional model forced by the astronomical cycle of solar heating and seasonal variation of surface meteorology derived from Bunker's climatology. The model is integrated for 18 months to show the seasonal modulation of the diurnal cycle. Nocturnal convection plays a dominant role. The convection depth closely follows the thermal compensation depth during the day when they are less than the turbocline depth. Integrating the model with a 24-hour time step leads to large errors in the seasonal variation of mixed layer temperature and depth, and in the source term of isopycnic potential vorticity. The errors are reduced by using two time steps per day, one for the daytime when convection is quenched, the other for the night when it is active. A novel parametrization based on tuning the daily equivalent solar elevation to surface temperature further reduces the error. This parametrization is used to investigate the sensitivity of the seasonal cycles of mixed layer depth and temperature to: (1) seasonality in the surface fluxes; (2) systematic changes in the net annual solar heating; (3) random changes in the seasonal cycles of solar heating induced (i) monthly and (ii) daily. The sensitivity to uncertainty in seawater turbidity is investigated in the same way. The profile of isopycnic potential vorticity subducted into the thermocline depends on the vernal correlation of mixed layer depth and density, so gyre circulation is sensitive to solar heating in spring.

1. INTRODUCTION

The response of the upper ocean to diurnal variation of solar heating has a long research history (Defant 1961). Interest in the subject has revived in recent years as climatologists have realized that failure to resolve or adequately parametrize the diurnal cycle in the upper ocean leads to systematic errors in the seasonal and longer term temperature and depth of the mixed layer (Woods 1984). It is desirable to avoid the short time steps needed to resolve the diurnal cycle in long term integrations of coupled ocean–atmosphere models designed to investigate climate change. The aim is to introduce into the model a parametrization that minimizes the errors in seasonal and longer term variations of mixed layer temperature and depth that result from failing to resolve diurnal variation. Successful parametrization requires a detailed understanding of the physical processes involved. The aim of this paper is to clarify the physics underlying the changes that occur in the mixed layer as the result of solar heating, and to present the results of sensitivity and parametrization studies.

The work is based on a one-dimensional model similar to those currently being

used in coupled ocean–atmosphere models (Nihoul 1985). It incorporates the slab parametrization of turbulent mixing introduced by Kitaigorodskii (1960) and used by Kraus and Turner (1967) in the first model of the seasonal cycle in the ocean. Several reviews of the method are available (e.g. Niiler 1975, 1977; Niiler and Kraus 1977). The slab parametrization has been widely used in models of upper ocean response to changes in the weather (Denman and Miyake 1973; Davis *et al.* 1981), to the diurnal cycle (Turner 1969), the seasonal cycle (Wells 1979; Gaspar 1985) and climate change (Gordon 1985).

The paper starts with a restatement of the physical processes involved in mixed layer dynamics incorporating recent advances. Next comes a description of the one-dimensional model used in this study. Then comes the result of running the model under a series of controlled conditions designed to reveal the mean diurnal seasonal cycles that the model predicts when forced by the astronomical cycle of solar heating, plus Bunker (1976) surface forcing at a location in the Atlantic where advective changes are relatively small. The next section shows the consequences of integrating the model with time steps too long to resolve the diurnal cycle and introduces a method to minimize the errors. Finally, we explore the sensitivity of the model to uncertainty in the solar heating profile.

2. Physics

(*a*) *Nomenclature*

The water column is divided into layers (Fig. 1). At the top is the convection layer in which heat flows upwards to supply the surface losses to the atmosphere. It is embedded in the mixed layer, which is continually turbulent. The bottom of the mixed layer is defined by the turbocline, below which turbulence is intermittent and on average very much weaker. The diurnal pycnocline lies between the turbocline and the top of the seasonal pycnocline which extends down to the top of the permanent pycnocline. The diurnal pycnocline disappears every night and the seasonal pycnocline every winter; the permanent pycnocline is always present. The water column is statically unstable (Brunt–Väisälä frequency N is imaginary) in the convection layer ($0 < z < C$) and statically stable ($N^2 > 0$) in the rest of the mixed layer ($C < z < H$), in the diurnal pycnocline ($H < z < H_{max}$), the seasonal pycnocline ($H_{max} < z < D$) and the permanent pycnocline ($z > D$). The change in density gradient at the boundaries between the layers, shown schematically in Fig. 1, is a feature of model integrations forced by the climatological mean diurnal and seasonal cycles. The values of C, H, H_{max} and D are equally well defined when the forcing is disturbed by changes in the weather and climate, but they are not then so clearly associated with features in the density profile. It is therefore desirable to avoid the practice of basing the nomenclature on the appearance of the density or temperature profile, which has led to confusion in the literature over the precise meaning of 'mixed layer depth' and 'Deckschichttiefe', and the introduction of variations such as 'mixing layer depth', 'potential layer depth' and 'transient thermoclines' (Tully and Giovando 1963). It must also be borne in mind that this paper is concerned with the one-dimensional structure of the upper ocean, and therefore does not take account of fine structure arising from intrusion of lateral inhomogeneities.

Seawater density depends on both temperature and salinity: at locations where the vertical salinity gradient is negligible the name 'pycnocline' can be replaced by thermocline. In the remainder of this section we shall assume the contribution of salinity changes is negligible. It will be considered briefly in the section on model results.

(*b*) *Solar heating*

Simpson and Dickey (1981a, b) have emphasized the importance of accurately

parametrizing the solar heating profile in models of the diurnal cycle in the upper ocean. They concluded that the two-exponential data fit of Paulson and Simpson (1977) is adequate for all purposes except very calm weather, when they suggested an abbreviated version (nine wavebands) of the 27-waveband spectral synthesis in Woods (1980). Woods, Barkmann and Horch (1984) showed that the Simpson–Paulson parametrization can lead to errors (in the data fit) of up to 30% and proposed a three-exponential parametrization which reduced the errors by an order of magnitude. They showed that the Woods spectral synthesis (for pure water) agreed well with that empirical parametrization in the case of Jerlov's optical type 1 seawater (very clear) in the top five metres of the ocean, and therefore advocated the use of the synthesis method to study mixing within the top few metres of the ocean. In this study we have adopted the Woods–Barkmann–Horch parametrizations, using the empirical or synthesis version as appropriate.

(c) *Convection*

The combination of evaporation, conduction and net long-wave radiation transfers energy from the ocean to the atmosphere at rate B. This heat loss is supplied by heat flowing up towards the surface from a depth C, the convection depth. The potential energy released as heat flows upwards appears as kinetic energy of convective overturning, with energy-containing eddies of height C, which power turbulence at a rate E_c given by

$$E_c = \int_0^C \varepsilon_c \, dz = \rho B C \alpha g / 2s \tag{1}$$

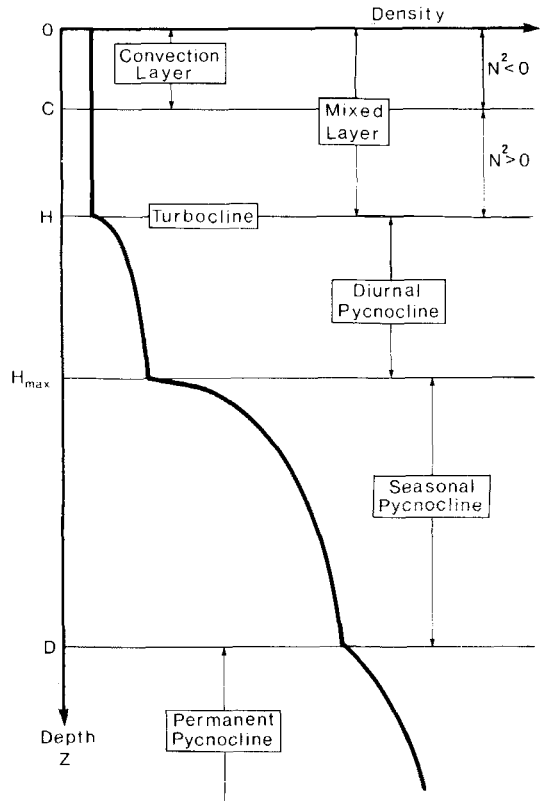

Figure 1. Nomenclature used in this paper.

where ρ is the density of seawater, α is the coefficient of thermal expansion, g is the acceleration due to gravity and $s = 4{\cdot}2\ \mathrm{MJ\ m^{-3}K^{-1}}$ is the specific heat of seawater. A small fraction m_c of that turbulent power input is consumed in entraining denser (colder) water from below the convection layer. The maximum possible value of m_c is 0·15 according to the flux Richardson number criterion of Ellison (1957), but there is experimental evidence that it may be smaller, especially when C is large (Killworth 1983). In the limiting case where $m_c = 0$ the convection is said to be non-penetrative and its depth C can be calculated simply by the method of convective adjustment (Turner 1973).

Solar heating has a profound effect on the depth of convection because it is concentrated close to the surface. Half of the solar energy is absorbed in the top metre of the ocean. For several hours centred on noon each day at most locations around the world, the oceanic heat gain from the sun is more than double the loss to the atmosphere. The depth of convection is then less than one metre, regardless of the depth of the turbocline, the latter normally being much more than one metre. At night the heat loss to the atmosphere is supplied convectively from heat stored during the day and, in the cooling season, during earlier days. The depth of convection then nearly reaches the turbocline defining the bottom of the mixed layer.

Woods *et al.* (1985) confirmed Woods's (1980) assertion that, because of the concentration of solar heating close to the surface, the thermal compensation depth C' provides an accurate surrogate for the convection depth C during the day, when it is much shallower than the turbocline. They showed that the results of Dalu and Purini (1982) which appeared to contradict it were an artifact of their oversimplified solar heating parametrization.

(*d*) *Turbulence*

One of the major advances in the past decade has been the reliable measurement of profiles of turbulent kinetic energy in the upper ocean (Oakey and Elliott 1982; Shay and Gregg 1984). Such measurements have made it possible to quantify the conceptual model of a vigorously turbulent mixed layer overlying a largely laminar flow thermocline, that had evolved from the appearance of temperature profiles (Defant 1936) and flow visualization studies (Woods 1968). The measured dissipation rate of turbulent kinetic energy, ε, is typically of order milliwatts per cubic metre ($\mathrm{mW/m^3}$) in the mixed layer and of order microwatts per cubic metre ($\mu\mathrm{W/m^3}$) in the seasonal thermocline. The turbocline across which ε changes by a factor of 100 to 1000 is clearly defined in measured profiles of $\varepsilon(z)$. A standard value of ε, say $10\,\mu\mathrm{W/m^3}$, can be used as a criterion to allocate a precise depth to the turbocline. Natural intermittency in the turbulence poses a sampling problem that is being overcome (Gregg *et al.* 1985), but it is premature to ask how accurately the measured $\varepsilon(z)$ profile and the turbocline depth, as defined above, compare with those predicted by models of the upper ocean based on diffusive and slab parametrizations respectively. The importance of the new measurements of $\varepsilon(z)$ is that we can now abandon dependence on temperature profiles for (unreliable) indication of mixed layer depth in field data.

Oakey and Elliott (1982) have shown on the basis of $\varepsilon(z)$ measurements that the power supply to the turbulence in the mixed layer from the wind is 1% of the work done by the wind against the surface stress, τ:

$$E_w = \int_0^H \varepsilon_w \, dz = 0{\cdot}01 U\tau \tag{2}$$

where U is the wind speed. Below the convection layer, solar heating creates a stable

temperature gradient and any mixing produces a downward heat flux. Note that the direction of the heat flux (up if $z < C$; down if $z > C$) is independent of the intensity of the mixing. And, during the daylight period when the surface irradiance $I > 2B$, the value of C is almost independent of the intensity of mixing (i.e. of wind speed), because it almost exactly equals C', which is totally independent of mixing. The downward heat flux in the portion of the mixed layer below the convection layer ($C < z < H$) weakens the turbulence in the mixed layer. If the mean flux Richardson number in the mixed layer is equal to the critical value of 0·15, then (2) suggests that the work done by the mixed layer turbulence against the buoyancy force is 0·0015 times the work done by the wind against the surface stress, a value consistent with estimates based on laboratory experiments (Phillips 1977a, b) and changes in ocean temperature profiles (Denman and Miyake 1973).

We now consider the effect of solar heating on the turbocline depth. Its effect on convection has already been taken into account by adjusting C, the depth of the convection layer. No distinction is made in the slab parametrization between the contributions to the turbulent power supply from convection and wind stress

$$E = E_c + E_w. \tag{3}$$

The turbocline depth is adjusted so that a specified fraction of E is consumed by doing work against the buoyancy force.

$$E_B = Rf_c \exp(-H/H_0)\,.\,E \tag{4}$$

where Rf_c is Ellison's critical flux Richardson number and H_0 is a scale depth which some authors (e.g. Wells 1979) argue should be equal to the Ekman depth,

$$H_0 = L_E = \pi(2K/f)^{1/2}, \tag{5}$$

in which the eddy diffusivity K is given by Richardson's formula

$$K = (E/\rho)^{1/3}H. \tag{6}$$

The depth of the turbocline is diagnosed by equating E_B to the change of potential energy required to make the density gradient equal to zero in the mixed layer ($0 \leq z \leq H$), i.e.

$$E_B = (g/\Delta t)\int_0^H \{\rho(z) - \rho_0\}z\,dz \tag{7}$$

where ρ_0 is the resulting mixed layer density (Niiler and Kraus 1977). During the forenoon, solar heating often stabilizes the water in the mixed layer sufficiently for E_B to be consumed in a progressively shallower layer. The turbocline depth is then diagnosed to become smaller. After noon, as solar heating weakens, a progressively greater depth range is needed to balance E_B, and the turbocline deepens. This diurnal variation of the turbocline depth, with a minimum at noon, is similar in principle to the seasonal variation, with a minimum at the summer solstice, in the pioneering paper of Kraus and Turner (1967). Gargett *et al.* (1979) and Gregg *et al.* (1985) have observed the forenoon rise of the turbocline in time series of $\varepsilon(z)$ profiles.

3. The model

The one-dimensional model used in the present study incorporates the slab parametrization of turbulence in the mixed layer. The model is conceptually similar to that

of Niiler and Kraus (1977) but differs structurally, in that the temperature and salinity are adjusted three times within each time step of integration to allow for the following processes:
(1) solar heating, using the parametrization of Woods, Barkmann and Horch (1984), with seasonally varying cloud cover derived by interpolation between Bunker's (1976) monthly mean values, and constant, homogeneous seawater turbidity;
(2) convective adjustment using seasonally varying surface heat and net water fluxes derived from Bunker and Worthington (1976) and Baumgartner and Reichel (1975); this step yields a value for convection depth C;
(3) turbulent mixing, according to the slab parametrization method with $m = 1{\cdot}2 \times 10^{-3} \exp(-H/100\,\mathrm{m})$; this step yields a value for the turbocline depth H, and reduces the density gradient to zero in the mixed layer, $z < H$. Monthly mean values of the cube of the wind speed, $\overline{U^3}$, were estimated from Bunker's values of the monthly mean $\overline{U}$ and variance $\overline{U'^2}$ of the wind speed by the formula $\overline{U^3} \approx \overline{U}^3 + 3\overline{U}\,\overline{U'^2}$, where $U = \overline{U} + U'$. (This is probably an underestimate, given the neglect of skewness, which was not recorded by Bunker.)

This intra-time-step sequence of changes to the temperature and salinity profiles does not include a term for the divergences of the fluxes of heat and (fresh) water carried by the large-scale geostrophic currents and transient flow patterns associated with the synoptic and mesoscale motions. The net annual heat flux map of Bunker and Worthington (1976) shows that advective flux divergence is an important factor in the North Atlantic, and Woods, Barkmann and Horch (1984) have shown that it dominates temperature changes in the seasonal thermocline at OWS 'C'. Nevertheless, we were forced to leave it out of our model when preliminary Eulerian calculations showed that it is not possible to determine the current adequately from oceanographic data, while Lagrangian calculations have shown that the seasonal catchment area of water passing through any given location is enormously broadened by the transient quasi-geostrophic motions (Woods 1985). In order to avoid errors arising from neglect of the geostrophic flux divergence term in the model we shall present results only for locations where the mean current is weak, the quasi-geostrophic turbulent kinetic energy density is relatively low and the net annual heat and water fluxes through the sea surface are close to zero. Such a site is located in the north-east Atlantic sector of the anticyclonic gyre at 41°N 27°W. (Lagrangian integration of the model has been used to investigate water-mass formation (Woods and Barkmann 1986.)

4. Results

The model described above was integrated with one-hour time steps for 18 months for the climatological seasonal forcing at 41°N 27°W. The integration was started at the end of the cooling season, when the mixed layer is the deepest (on day 90). The initial temperature and salinity profiles had no vertical gradient down to the annual maximum mixed layer depth D for that location (obtained from Robinson *et al.* (1979)) and constant gradients in the permanent pycnocline below D (from the same source).

(*a*) *Diurnal variation*

Figure 2 shows the diurnal response of the convection depth C, turbocline depth H, mixed layer temperature T_0, and convective power supply to the turbulence in the mixed layer E_c. The daytime quenching of convection in the mixed layer and consequent reduction of power supply to turbulence are essentially as predicted by Woods (1980) on the basis of the diurnal variation of thermal compensation depth. The diurnal variation

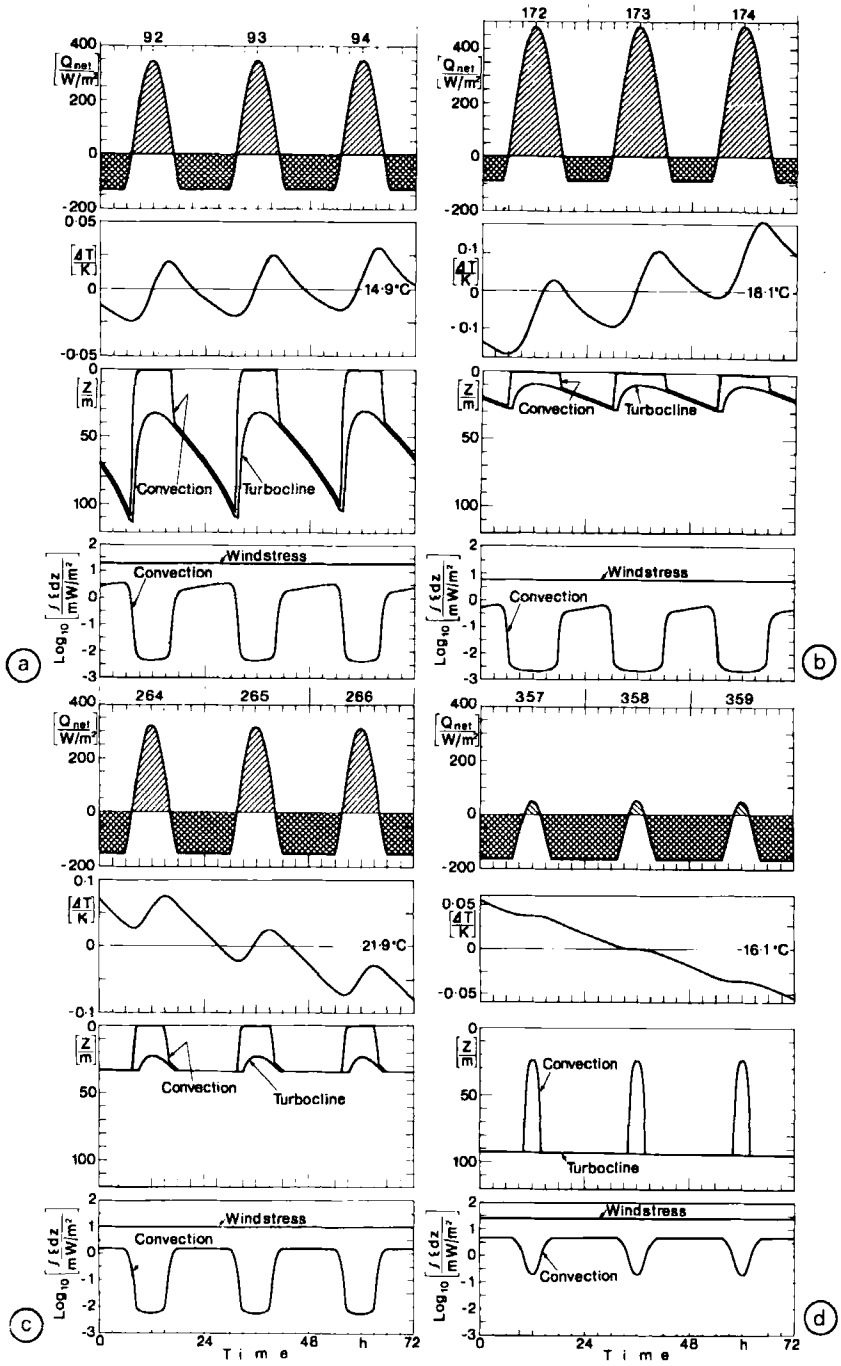

Figure 2. Diurnal variations of net surface heat flux, mixed layer temperature, convection and turbocline depths and power supply to mixed layer turbulence from convection and the wind stress, calculated for three days, using climatological mean surface meteorology derived from Bunker's (1976) monthly-mean data set. (a) Spring. (b) Summer. (c) Autumn. (d) Winter.

of turbocline depth is largest in the early spring, when it ranges between $H_{min} = 35$ m at noon to $H_{max} = 115$ m at the moment when the rising sun first heats the ocean faster than the surface heat flux to the atmosphere; or, allowing for salinity changes, when the net surface buoyancy flux changes sign, about an hour after sunrise. The temperature gradient at the top of the diurnal thermocline is still small at this time of year, so this large diurnal change of H is not easily detected in temperature profiles. It may therefore come as something of a surprise to oceanographers whose experience has been based on bathythermograph data. It is confirmed by measuring $\varepsilon(z)$ with microstructure profiles (Gregg *et al.* 1985).

(*b*) *Seasonal variation*

The seasonal modulation of the diurnal variation of turbocline depth is shown in Fig. 3. The diurnal range $H_{max} - H_{min}$ has a maximum at the start of the heating season, when the daily heat input from the sun first exceeds the surface heat loss; or allowing for seasonal changes in the surface water flux, when the net daily surface buoyancy flux changes sign. The diurnal range disappears in autumn, when the heat loss to the atmosphere is so large that (although it is exceeded by solar heating for a brief period around noon) the rate of potential energy gain from solar heating in the mixed layer remains less than E_B.

The seasonal variations of temperature, salinity and density profiles are shown in Fig. 4. Most of the seasonal heat and freshwater contents are stored in the top 50 m until the autumn when they are mixed deeper.

Figure 5(a) shows the seasonal variation of the daily minimum and maximum depth of the turbocline (consistent with Fig. 3), plus the depths of selected isotherms. The depth at which each isotherm is subducted during the vernal ascent of the (daily maximum) mixed layer depends on the correlation of the mixed layer depth and temperature, the isotherm being vertical at the moment of subduction. If there were no solar heating inside the seasonal thermocline the isotherms in Fig. 5(a) would appear horizontal after subduction. The rate of deepening due to internal heating reaches a maximum close to the summer solstice (any lag being due to seasonal variation of cloud cover or seawater turbidity). Individual isotherms deepen at different rates according to the variations of

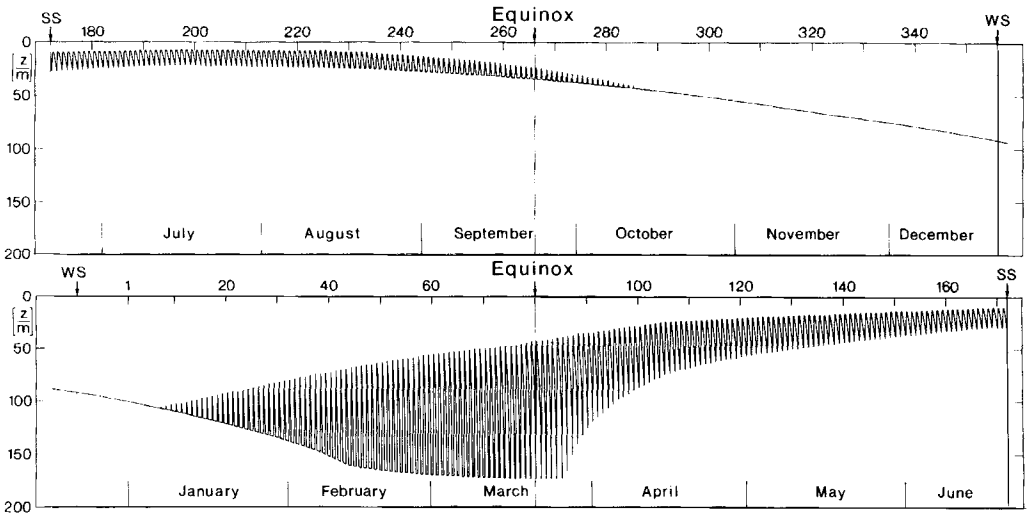

Figure 3. Climatological seasonal-mean modulation of the diurnal cycle of turbocline depth at 41°N 27°W calculated from the monthly-mean surface meteorology of Bunker and Worthington (1976).

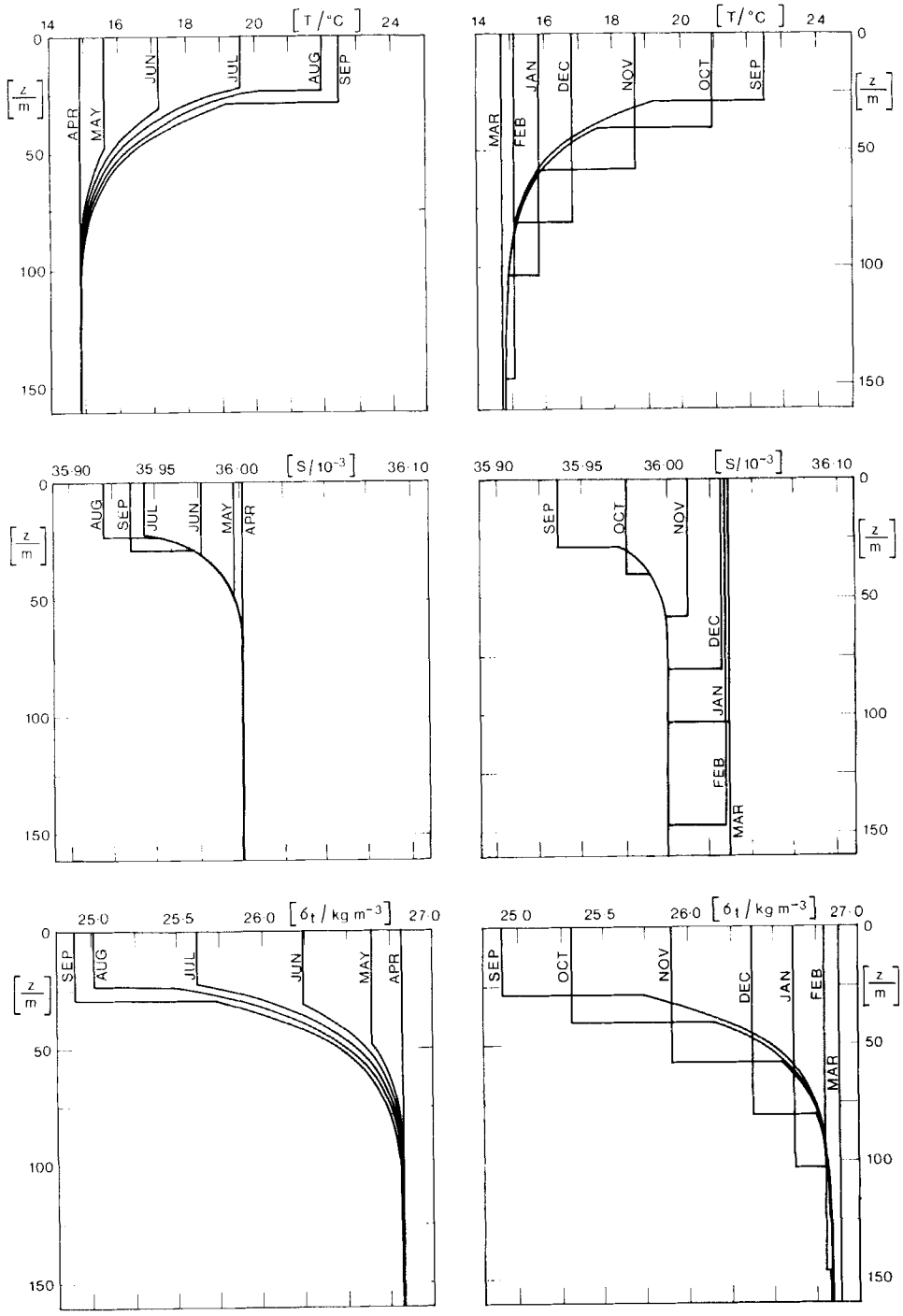

Figure 4. Mid month profiles of temperature, salinity and density, calculated with one-hour time steps using the astronomical variation of solar elevation, Bunker surface meteorology interpolated to daily values and Baumgartner and Reichel precipitation.

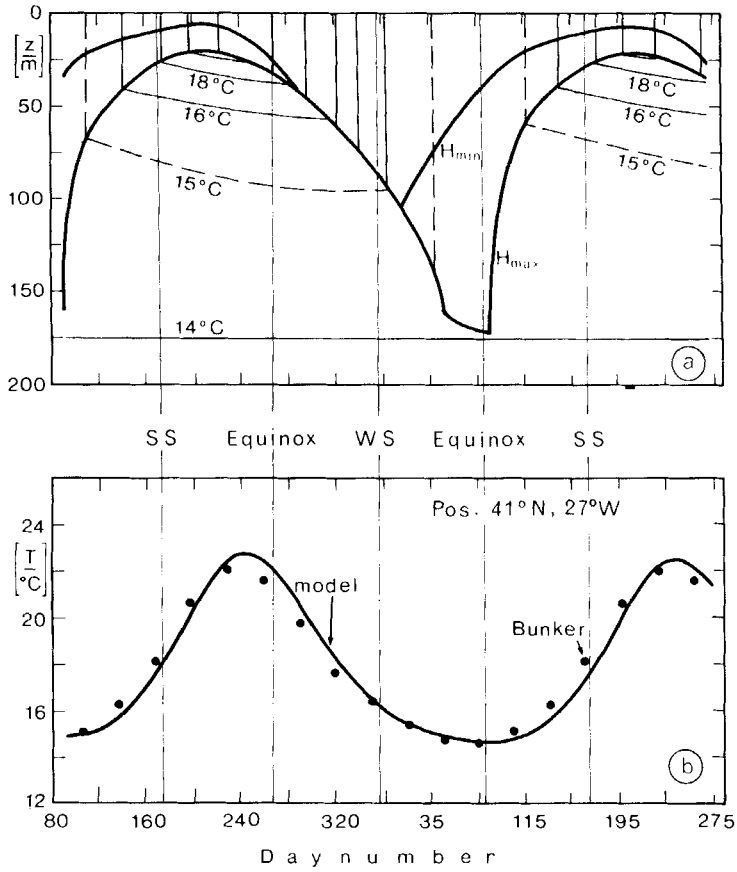

Figure 5. (a) The annual cycles of daily minimum and maximum turbocline depth, and the depth variation of selected isotherms. (b) The annual cycle of mixed layer temperature predicted by the model (line) and the Bunker (1976) climatological mean values. The observed good fit between model and data was achieved in part by selecting Jerlov type 1 for the constant seawater turbidity.

solar heating and temperature gradient with depth, the spacing between pairs of isotherms in the seasonal thermocline is thus changed each day between the dates of subduction in spring and re-entrainment next autumn or winter. At the chosen site water in the seasonal thermocline (i.e. below the Ekman layer) is displaced (geostrophically) less than 5° of latitude per year according to Sarmiento (1983). So: (1) the planetary vorticity of particles in the seasonal thermocline does not change significantly between subduction and re-entrainment; and (2) there is little change in the seasonal cycle of solar heating along the track of the particles. The change of spacing between pairs of isotherms predicted by this Eulerian integration of the model therefore indicates the diabatic change of isopycnic potential vorticity in the seasonal thermocline. (See Woods and Barkmann (1986) for the extension to strong geostrophic flows.)

The temperature profiles in Fig. 4 are characterized by a large change of temperature at the turbocline during the cooling season when the mixed layer is deepening. This appears in Fig. 5(a) as a trapping of isotherms in the descending turbocline from the moment when they are first captured to some weeks later when the isotherm rises vertically through the mixed layer showing that the latter has finally cooled to that temperature. This effect is independent of the diurnal cycle of turbocline depth, which disappears during the autumn (examine the 15 °C isotherm in Fig. 5(a)).

Figure 5(b) shows a comparison between the mixed layer temperature predicted by the model and the monthly mean values in Bunker's data. The value of seawater turbidity used in this integration (Jerlov type I) was chosen to minimize the difference between those surface temperature values. The residual errors, an overestimate of annual maximum temperature by 0·4 K and a lag of about one week in the cycle, might be attributed to neglect of temporal and vertical variations of seawater turbidity. The errors may also be the result of uncertainty in the Bunker surface meteorology used to run the model or in the Bunker surface temperatures. The sensitivity of the model to such uncertainties will be discussed later.

(c) *Modelling the seasonal cycle with longer time steps*

It has been shown above that the upper ocean responds strongly to the daily reversal in the surface buoyancy flux. In order to model the mixed layer and thermocline in a physically realistic way it is necessary to resolve the diurnal cycle of solar heating even if the aim is to simulate changes over much longer time scales. Here we concentrate on the seasonal cycle, which is fundamental to any discussion of climate change. For some applications it is unnecessary to model all the details of the diurnal cycle. For example, the diurnal modulation of mixed layer depth and temperature may be insignificant in modelling interannual climate change. When that is the case it may be possible to parametrize the physical processes associated with the diurnal cycle and to save computation time by using a longer step. In this section we report the results of an investigation designed to reveal the errors resulting from integrating our model for 18 months with time steps longer than one hour.

The integration described in the previous section was used as the standard for estimating the error introduced by adopting a longer time step. The investigation involved repeating the integration described in Figs. 3 to 5 with three different time steps: (1) twenty-four hours, (2) twelve hours centred on noon and midnight, and (3) two time steps per day centred on noon and midnight but varying in length seasonally according to the thermal compensation depth parametrization proposed in Woods (1980).

Particular attention was paid to the specification of the solar heating. In each case the daily heating profile was made identical to that in the standard run so that any differences arose from the impact of time step changes on the convection and turbulent aspects of the model. The results of the tests with 12- and 24-hour time steps are shown in Fig. 6. Both time steps yield a mixed layer that is too deep and too cold at all seasons, as was reported by Garwood (1979). This difference arises from a variety of non-linearities in the model. Firstly, convective adjustment changes both heat content and potential energy, so the diagnosis of turbocline depth following turbulent entrainment is sensitive to the number of time steps in 24 hours; secondly, the conversion of kinetic energy into potential energy by turbulent entrainment is a function of turbocline depth; and, thirdly, the diurnal quenching of convection by solar heating is not resolved in either the 24- or 12-hour time step integrations.

The 24 h time step gives a mixed layer that is about 10 m too deep in summer and 50 m too deep at the end of the winter. Comparison with Fig. 5 shows that this is equivalent to a 30% overestimate in mixed layer depth. The error extends through the spring heating season when the properties of the seasonal thermocline are being established. The error in mixed layer temperature increases through the heating season to a maximum at the solstice, about two weeks after the maximum sea surface temperature in the standard run. The maximum error is 1·5 K.

The errors in summer mixed layer depth and temperature with 12-hour time steps are about a third of those with 24-hour steps, but the depth of the mixed layer is still

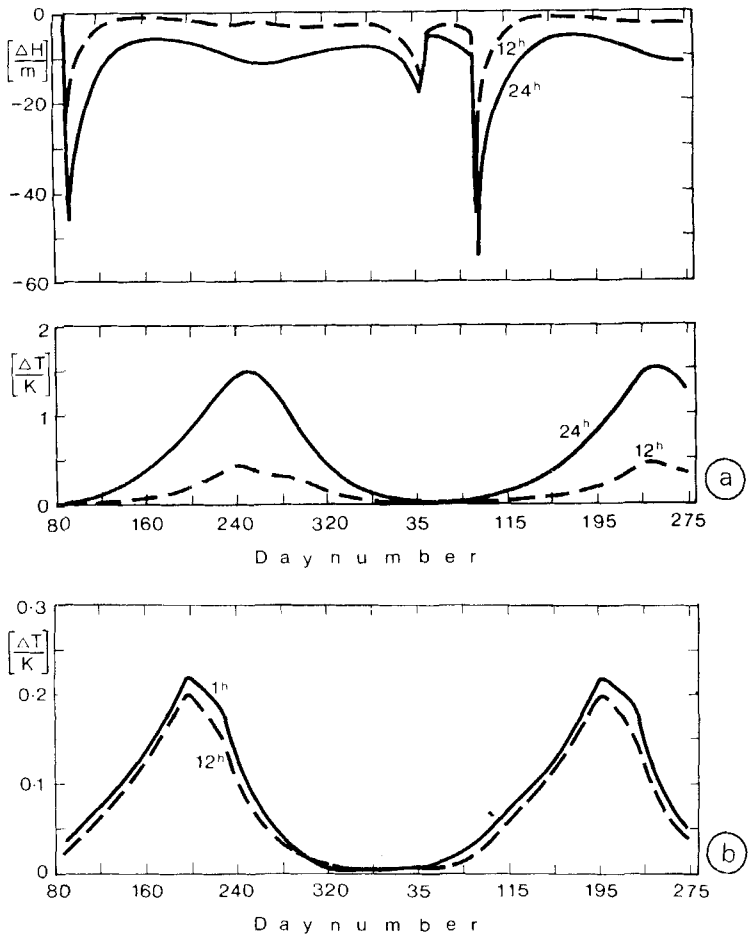

Figure 6. (a) The errors in the annual cycles of mixed layer depth (upper panel) and temperature (lower panel) arising from using time steps of 12 h (dashed curve) and 24 h (solid curve) instead of a time step of 1 h. (b) The seasonal variation of diurnal range of mixed layer temperature calculated with time steps of 1 h (solid curve) and 12 h (broken curve).

overestimated by more than 40 m towards the end of winter, and the errors in the correlation of mixed layer depth and temperature during the vernal ascent of the turbocline still leads to serious problems in predicting potential vorticity. The more sophisticated division of the day into two time steps adjusted according to the thermal compensation depth did not produce significant reduction in these errors. The diurnal range of mixed layer temperature is smaller in the integration with 12-hour time steps than in the standard (Fig. 6(b)).

Having investigated the impact of longer time steps on the model given identical daily solar heating profiles, we decided to investigate the possibility of reducing the errors in the seasonal variation of mixed layer depth and temperature by modifying the solar heating profile according to the length of the time step. In this case we used the solar radiation routine in the model to determine the heating profile for each time step (regardless of its length) given a prescribed value for the solar elevation. In the standard integration with one-hour time steps we specified the solar elevation astronomically as in Fig. 5. For the 12- and 24-hour time step integrations we had to decide on an equivalent

refraction angle, α^*. That gave the opportunity to introduce a parameter that could be tuned to minimize the errors in predicted mixed layer depth and temperature. The determination of a value for the equivalent refraction angle for each day of the year was done in two steps. First we calculated a mean refraction angle $\bar{\alpha}$ for each day of the year (at the chosen location) weighted by the instantaneous surface irradiance, $I(0)$:

$$\bar{\alpha} = \sum_{j=1}^{k} \alpha_j \, . \, I_j(0) \Big/ \sum_{j=1}^{k} I_j(0). \tag{8}$$

The value of the refraction angle used in the model was

$$\alpha^* = \bar{\alpha} + \alpha' \tag{9}$$

where the parameter α' was determined by comparing the annual maximum (September) sea surface temperature in the standard and longer time step integrations (Fig. 7). The best fit value of α' for each choice of time step was then used as a constant parameter throughout the annual integration.

This parametrization led to a significant reduction in errors in both the depth and temperature of the mixed layer. Difference plots are shown in Fig. 8. The summer mixed layer depth is less than five metres too deep in the 12-hour integration and less than ten metres too deep in the 24-hour integration. The much larger errors (40 to 50 m) at the end of winter are due to phase shift, which will be discussed in the next section. The errors in mixed layer temperature are around ±0·1 K and ±0·3 K for the 12 h and 24 h time steps respectively. The diurnal range of mixed layer temperature is predicted to within 0·05 K by the 12 h time step integration, and apart from a large winter error due to phase shift the diurnal range of mixed layer depth is within 10 m of the standard run. We conclude that tuning the solar elevation offers an effective and economical way to reduce errors in modelling the seasonal cycle with time steps too long to resolve the

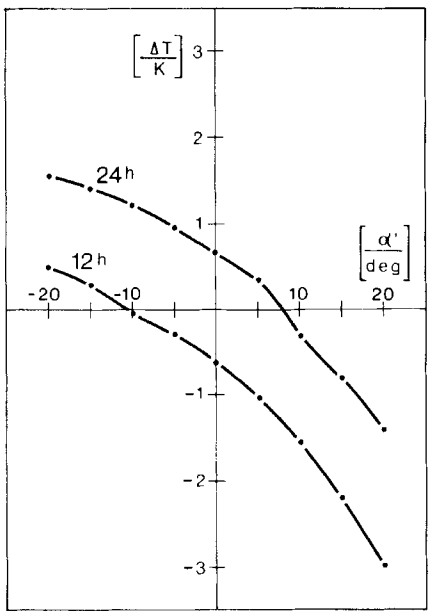

Figure 7. Tuning diagram for the parameter α', showing its variation with the error in mixed layer temperature for time steps of 12 h and 24 h.

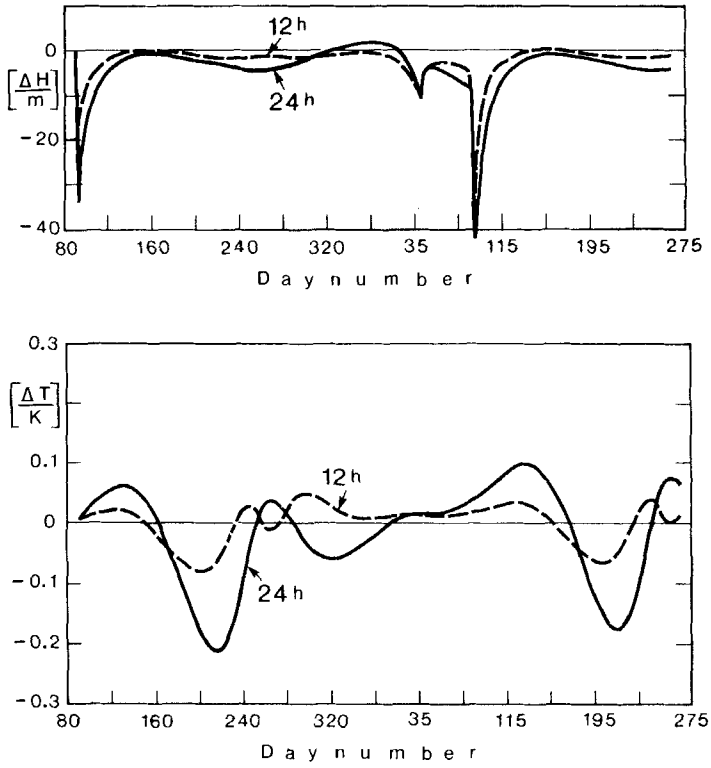

Figure 8. As Fig. 6(a), but based on solar elevation parametrization.

diurnal cycle. The calculations were repeated for a site (59°N 31°W) where the seasonal variation of day length is much stronger; the resulting error in surface temperature was even smaller than at the standard site (41°N 27°W).

The correlation of mixed layer temperature and depth during the vernal ascent of the turbocline determines the source of isopycnic potential vorticity (Q_s) in the seasonal pycnocline, and eventually in the permanent pycnocline (Woods 1985). The errors in the 24 h time step integration (Fig. 9) lead to a significant error in the potential vorticity injection and would therefore have serious consequences for calculations of ventilation of the wind-driven gyres. The error is greatest during the early part of the heating season, when the densest layers are subducted. Woods (1985) has shown that these are the layers that are most likely to flow into the permanent pycnocline, so the error arising from using longer time steps is worst where it can do most damage to predictions of gyre circulation. Note that this error in Q_s is *not* due to the winter phase lag which leads to large differences in mixed layer depth (Figs. 6(a), 8). The error is reduced by using two time steps per day and solar elevation parametrization (Fig. 9).

(*d*) *Sensitivity of the seasonal cycle to uncertainty in solar heating profile*

The predictability of mixed layer temperature and depth is limited by the errors in data used to run the model. In this section we report the results of tests designed to discover the effect of uncertainty in the solar heating, concentrating on the two variables of greatest importance (Woods, Barkmann and Horch 1984): cloud cover and seawater turbidity.

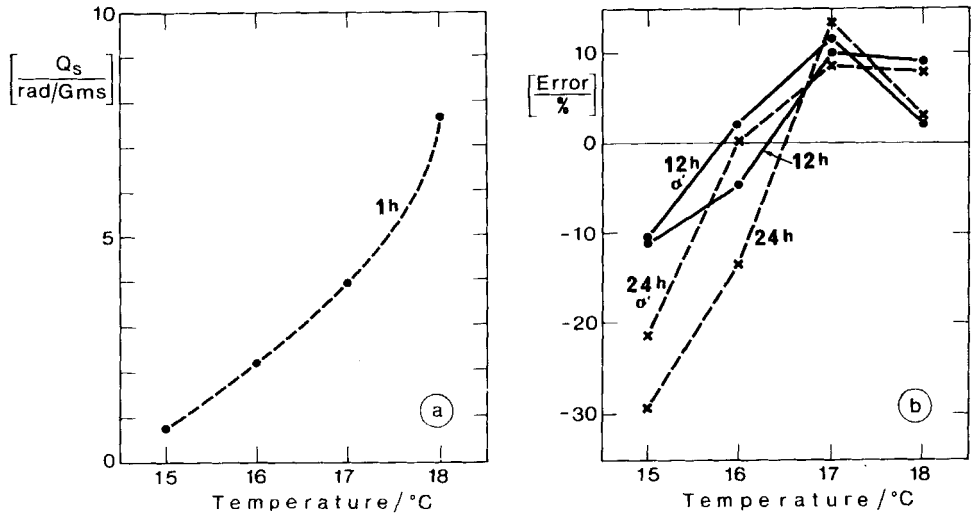

Figure 9. (a) Source term of isopycnic potential vorticity (Q_s) from Fig. 5. The Q_s values refer to layers bounded by isotherms half a degree colder and warmer than the indicated value. N.B. isotherms and isopycnics coincide in the seasonal thermocline (i.e. it is thermotropic) because salinity variations were neglected in this integration. (b) The percentage error in Q_s due to using longer time steps as in Fig. 6 (heating profile parametrization) and Fig. 8 (solar elevation parametrization, indicated by 'α'').

The earliest model of the seasonal cycle (Kraus and Turner 1967) was forced by a sinusoidal variation of surface irradiance, all other forcing being kept constant. Throughout this investigation, we have used astronomical variation of solar elevation plus Bunker's (1976) climatological forcing, which includes the seasonal variations of cloud cover, wind stress and oceanic cooling to the atmosphere. In order to discover the role played by these seasonal variations of surface fluxes we compared the seasonal cycle of mixed layer temperature predicted by the model with one of the three variables (cloud, wind or cooling) held constant throughout the year. In the case of the runs with constant cloud and constant cooling the values were chosen to produce the same annual heat budget. The results are shown in Fig. 10. At the chosen site (41°N 17°W) the effect of seasonality in cloud cover is relatively small. Neglecting the seasonality in surface cooling produced an error of 3 K and a half-month delay in the annual maximum temperature.

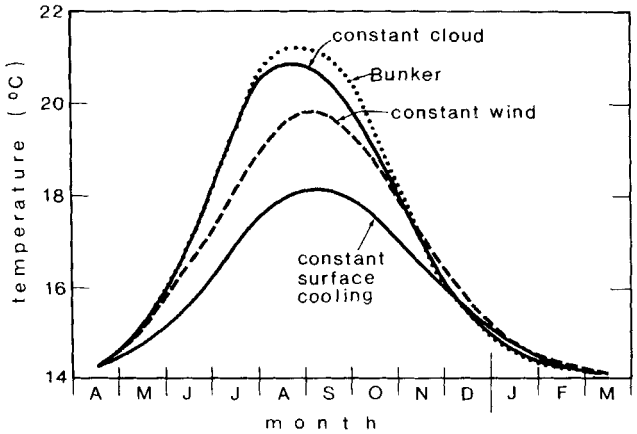

Figure 10. Sensitivity to seasonality in cloud cover, windstress and surface cooling.

Neglecting seasonality in the wind stress produces an error of the same sign, but only half the amplitude. We conclude that it is twice as important to describe the seasonal cycle of the surface buoyancy flux as the seasonal cycle of the wind stress if the aim is to predict the annual cycle of surface temperature.

The next set of tests explored the sensitivity to uncertainty in the solar heating. Three time scales are considered: (1) one year; (2) one month; and (3) one day. The first provides some insight into the sensitivity of sea surface temperature (as predicted by our model) to secular changes of surface forcing due for example to increasing concentration of carbon dioxide in the atmosphere. The second is particularly relevant to prediction of interannual anomalies of sea surface temperature with monthly-mean data such as are specified for the TOGA programme (WMO 1984). The third reveals the sensitivity of the mixed layer to random changes of weather as a function of season. Our aim was to discover the impact of experimental errors in solar heating on these three time scales, paying attention both to systematic biases and to random errors. In that context it is worth noting the state of the art of measuring the variables relevant to solar heating (reviewed in Woods (1984)). Monthly-mean solar irradiance can be estimated from satellite data to $\pm 10\,W/m^2$ (Gautier 1984), which compares favourably with the experimental errors of $\pm 30\,W/m^2$ in surface cooling calculated from merchant ship data. Systematic biases in experimental values of surface fluxes cannot be estimated directly because of errors of both measurement and sampling in the precision data sets used for comparison. However, there is indirect evidence of bias from large-scale budget studies (e.g. Bunker *et al.* 1982). We shall see that these uncertainties in the surface forcing lead to large errors in the mixed layer temperature and depth predicted by our model.

The first test comprises 30 independent annual integrations starting from the same initial conditions and using the Bunker climatology (as in Fig. 5) but with different sequences of random fluctuations in the cloud cover every time step. For economy we used a time step of twelve hours with solar elevation parametrization, which was shown earlier to capture the main features of the seasonal cycle. Figure 11 shows the variations of mixed layer depth (daily minima and maxima) and temperature for one of the runs.

One of the consequences of the random fluctuations in cloud cover was an accumulated difference in the total input of solar energy integrated over the year. This has an impact on the deepening of the mixed layer in winter. In all runs the maximum depth of the mixed layer at the end of the winter exceeded the depth (160 m) at the start of the integration. There is little point in analysing the differences in the annual maximum depth of the mixed layer achieved in each of the thirty runs, because they depend on the initial thermocline stratification and in the real world the annual maximum depth of the mixed layer is controlled by advection, which we neglect in this study (see Woods 1985). We therefore focus on phase changes in the winter descent of the mixed layer, while it is still independent of initial conditions. Figure 12 shows the day on which the mixed layer depth first exceeds the initial value, as a function of the annual input of solar energy. The regression line has a slope of nearly 4 days per W/m^2. That variation of the surface short-wave flux might be due to clouds or to dust from volcanoes or nuclear bombs. It also provides a rough estimate of the response to changes of long-wave flux resulting from carbon dioxide pollution of the atmosphere, which is expected to be about $1\,W/m^2$ per decade. The fluctuations about the trend line (standard deviation approximately three days) arise from the method used to create the different annual energy inputs. They will be discussed below.

The same approach is followed in studying the sensitivity of the mixed layer temperature to randomly generated changes in the integrated solar energy input. In this case the mean heating anomaly is calculated from the start of the integration (day number

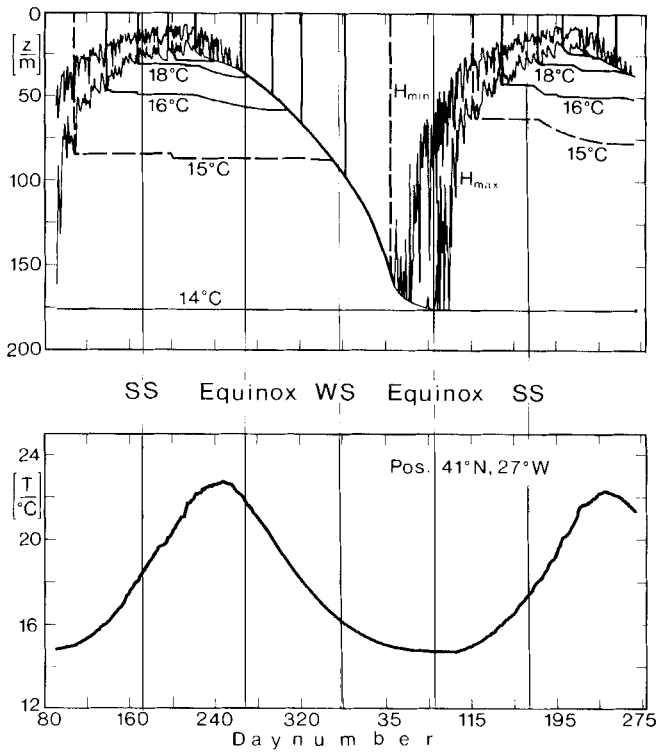

Figure 11. As Fig. 5, but with random variation of cloud cover every day.

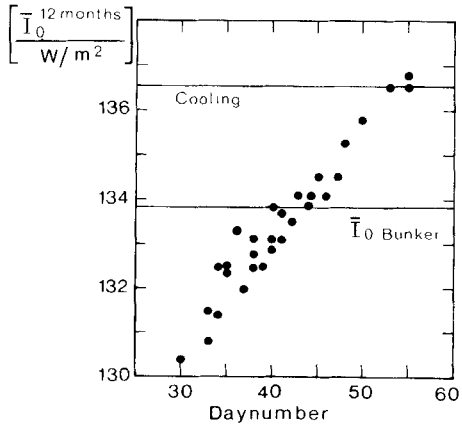

Figure 12. Correlation between annual energy budget and date on which the mixed layer first descended below 160 m. The Bunker climatological values for solar heating and cooling to the atmosphere are indicated by horizontal bars, showing that Bunker predicts a net heat loss of 2·7 W/m^2 per year at this site (41°N 27°W).

90) to the 15th day of the month for which the temperature anomaly is calculated. For example, Fig. 13(a) shows the variation of temperature and integrated irradiance anomalies for September in the thirty runs with different sequences of random fluctuations of cloud cover. That analysis was repeated for every month of the year. The results are summarized in Fig. 13(b). Curve 'b' shows the seasonal variation of sensitivity of the mixed layer temperature to accumulated solar heating anomaly; the sensitivity is greatest in summer when the turbocline is shallow. The maximum scatter in mixed layer temperature for the 30 integrations is nearly 1 K, but after removing the trend with accumulated heat content it reduces to 0·3 K. For comparison we include the systematic change in mixed layer temperature arising from a steady increase of 10 W/m^2 in solar heating over the Bunker values used in the standard run.

The probability distributions for the errors in mixed layer depth and temperature produced by the random fluctuations of cloud cover in the thirty independent integrations are shown in Fig. 14(a). For comparison Fig. 14(b) shows the corresponding probability distributions for thirty integrations of the model with the random fluctuations in the

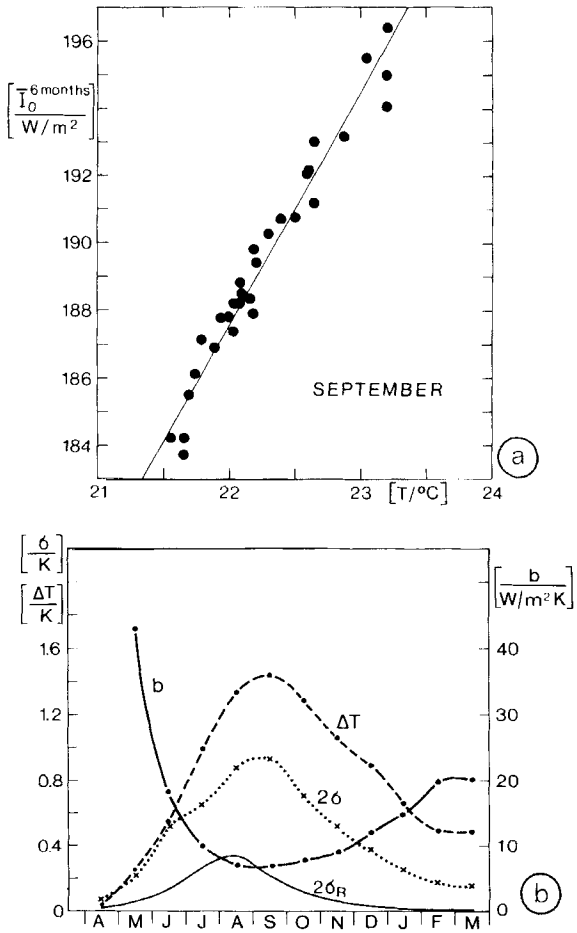

Figure 13. (a) Correlation between integrated solar heating and mixed layer temperature in mid September. (b) Seasonal variation of the sensitivity of surface temperature to integrated solar energy input 'b', the increase in mixed layer temperature for a steady increase of 10 W/m^2 in solar heating, the total scatter in mixed layer temperature (2σ) and the residual scatter after removal of the systematic trend with accumulated energy input ($2\sigma_R$).

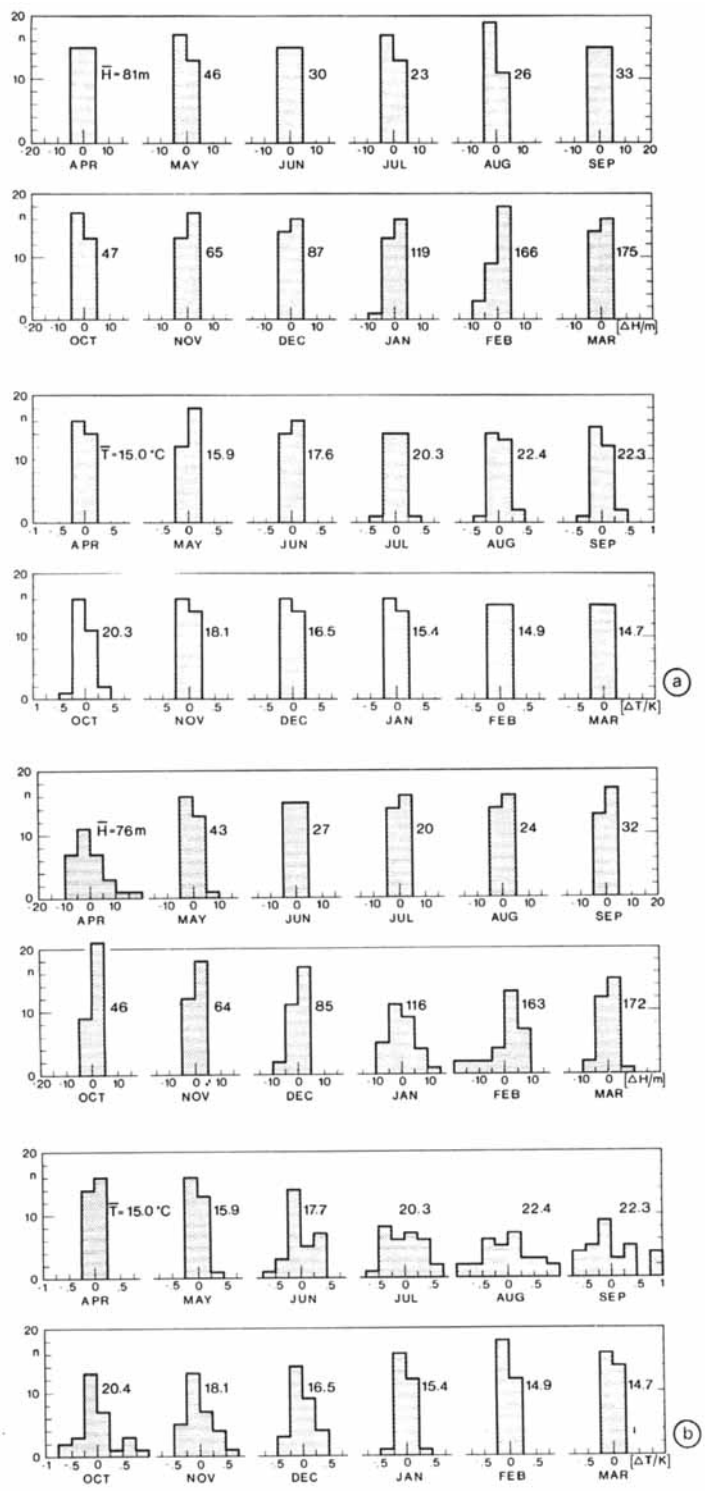

Figure 14. Probability distributions for mixed layer depth and temperature for each month of the year based on: (a) 30 runs in which the monthly mean solar energy input deviated from the Bunker values by a random amount in the range $\pm 10\,W/m^2$; (b) 30 runs in which the cloud cover (in tenths) deviated every day from Bunker's seasonal value C_B (month) by random amounts in the range $(2C_B - 10)$ to 10.

range $\pm 10\,W/m^2$ (top hat distribution) on the Bunker monthly mean climatological cloud cover (applied before the interpolation which gives values at every time step).

(e) *Sensitivity to seawater turbidity*

The solar heating profile is sensitive to seawater turbidity, about which we have only the sketchiest knowledge (Woods, Barkmann and Horch 1984). There is scope for large uncertainty in the climatological mean seasonal cycle of turbidity, and in rapid fluctuations associated with patchy development of plankton in response to transient eddies and fronts in the upper ocean. Charlock (1982) has shown that a mixed layer model (incorporating a simple parametrization of solar heating and not resolving the diurnal cycle) is sensitive to turbidity. All integrations so far reported in this paper have been made with constant seawater turbidity corresponding to Jerlov (1976) optical type 1, which yielded the best fit of mixed layer temperature to Bunker data at the test site (see Fig. 5). Figure 15(a) shows the sensitivity of the annual cycle of sea surface temperature to assumed value of the turbidity, held constant throughout the year. Errors of over 1 K can easily be attributed to uncertainty in the turbidity of ± 1 unit on the Jerlov scale, which is about the level of our ignorance for the mean annual value. The corresponding error in annual cycle of mixed layer depth is shown in Fig. 15(b). Normally the turbidity is not constant, but increases to a maximum during the phytoplankton bloom which follows the vernal rise of the turbocline (Woods and Onken 1982). This seasonal variation in turbidity increases the scope for errors in the model-predicted surface temperature. The results of a preliminary study (Fig. 15(c)) show that the mixed layer temperature is much more sensitive to the spring bloom than to the secondary bloom in the late summer; it is even more sensitive to high turbidity in summer, but that is hindered by nutrient depletion except in upwelling regions.

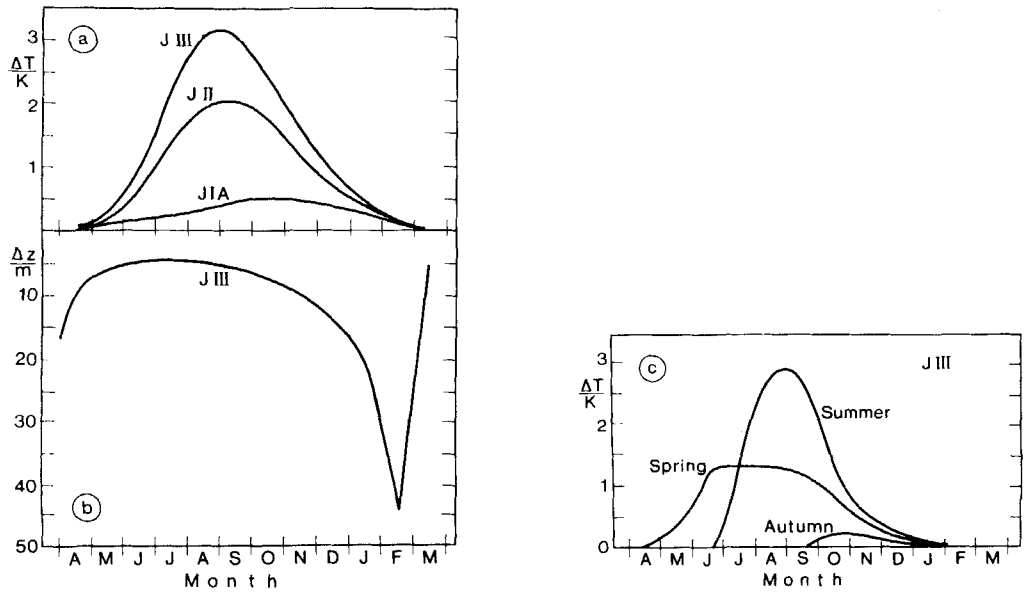

Figure 15. Sensitivity of mixed layer temperature and depth to uncertainty in seawater turbidity. (a) Mixed layer temperature anomaly relative to annual cycle for clear water ($J = 0$) for three optical water types (JIA, JII, JIII). (b) Mixed layer depth anomaly for Jerlov optical type III relative to clear water. (c) Sea surface temperature anomaly due to a plankton bloom with Jerlov type III occurring at different seasons: (i) spring, (ii) summer, (iii) autumn.

With that background we proceeded to undertake a sensitivity study like that reported above for cloud cover. The standard run was an 18-month integration at the standard site under standard conditions (12-hour time steps using solar elevation parametrization) with Bunker forcing and optical water type 1. Two sets of thirty test runs with random fluctuations in the turbidity were then made and compared with the standard run. In the first set (Fig. 16(a)) the random fluctuations were applied at monthly intervals: in the second set (Fig. 16(b)) the fluctuations were applied at every time step. In both cases the fluctuations were distributed in a top hat distribution in the range $2{\cdot}25 \pm 1{\cdot}45$ units of colour index (see Jerlov 1976). The parameters in our solar heating profile scheme were interpolated between the discrete Jerlov values using the colour index. It is concluded that the largest errors arise in July to October especially when the uncertainty occurs in the monthly mean.

5. Discussion

The results presented above were obtained using a one-dimensional model of the seasonal boundary layer of the ocean incorporating Kraus–Turner diagnosis of the mixed layer depth. Models of this type have been the subject of many investigations and are being incorporated into atmospheric general circulation models with a view to generating realistic interannual anomalies of sea surface temperature. Woods (1984) pointed out that this application of the technique is premature, given the inability of existing models to predict sea surface temperature to better than ± 1 K, an error comparable with the interannual anomalies. There is a need to investigate the source of these errors, by sensitivity studies, and by comparison with field data.

This paper has reported the results of sensitivity tests related to problems arising from the largest term in the surface forcing, solar radiation. A reference model designed to resolve the effects of solar heating in the seasonal boundary layer was constructed using spatial and temporal resolutions too extravagant for inclusion in general circulation models. Investigation of the properties of that reference model led to predictions that suggest more effective experimental tests than have been achieved hitherto; they will be discussed below. Sensitivity studies were based on comparison with the seasonal cycle of mixed layer properties predicted by the reference model. The first tests investigated the consequences of adopting longer time steps, as will be necessary in climate models. A novel parametrization, based on solar elevation, seemed to offer the best solution. That was used to investigate the sensitivity of the seasonal cycle (predicted by a version of the model with two time steps per day) to uncertainty in the two factors that most affect the profile of solar heating, namely cloud cover and seawater turbidity.

These sensitivity studies make it clear that, regardless of any doubt concerning the formulation of the model, there will always be errors in the predicted mixed layer temperature and depth, and in the source term for isopycnic potential vorticity, simply because of uncertainty in the solar heating profile. In our opinion there has been too much discussion in the literature about the finer points of model parametrization, and too little about the inevitable errors associated with uncertainty in the forcing terms. Hofmann (1982) investigated the sensitivity to uncertainty in wind speed. The results presented in this paper quantify the errors due to uncertainty in the solar radiation. Climate modellers may need to revise their expectations about the likely gain from incorporating a mixed layer model into atmospheric general circulation models and, in the future, into coupled models of atmospheric and ocean circulations. The error in source term of isopycnic potential vorticity is of primary importance for coupled circulation models.

However, it would be wrong totally to neglect errors arising from the detailed construction of the model. We have drawn attention to the inherent non-linearity of our model. It is sensitive to the order of the intra-time-step sequence of operations (solar heating, convective adjustment, turbulent entrainment); the error increases with the length of time step. There are also problems associated with the rather crude reduction of effective Richardson number with turbocline depth: that point is considered in part II (Woods and Strass 1986). More fundamentally, it might be argued that our use of Kraus–Turner parametrization is significantly inferior to the higher-order closure schemes reviewed by Mellor and Yamada (1982). Here we can refer to the detailed examination of mixed layer variation predicted by our reference model, which resolves the diurnal response to solar heating. The striking diurnal variation of mixed layer depth (Figs. 2, 3) offers a target for experimental tests of the model that has not hitherto been exploited. A detailed comparison with a diurnal time series of high quality oceanographic data collected during GATE (Pirotton 1985) will be the subject of a future publication.

Recent advances in techniques for measuring the vertical profile of turbulence in the upper ocean (e.g. Oakey and Elliott 1982; Kitaigorodskii *et al.* 1983) encourage us

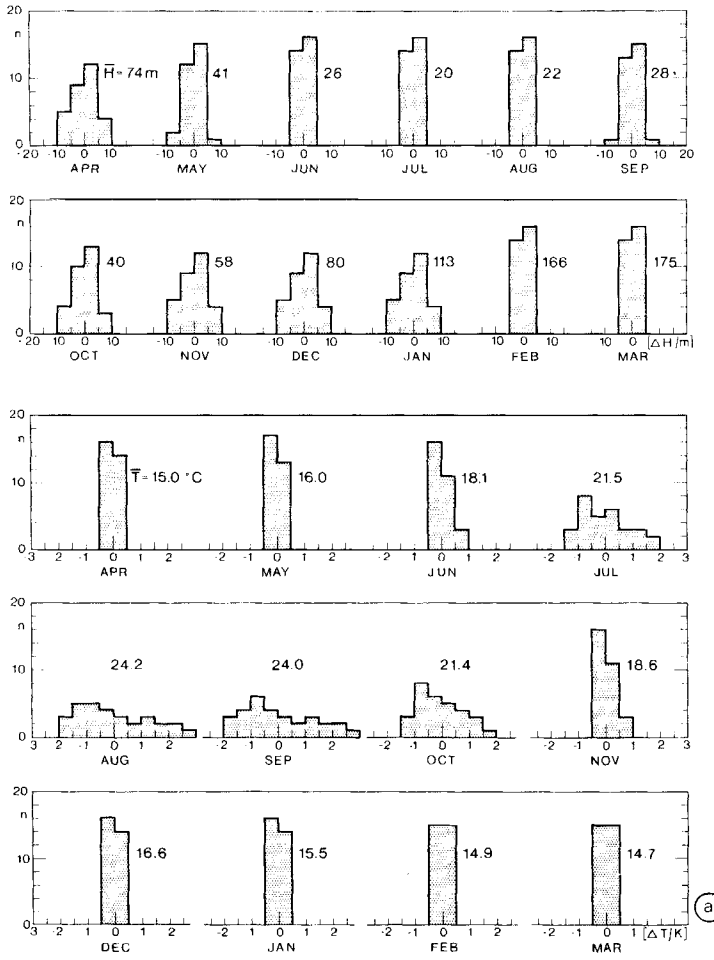

Figure 16. Probability distributions for mixed layer depth and temperature for each month of the year based on: (a) 30 runs in which the monthly-mean colour index was varied randomly in the range 2·25 ± 1·45, before interpolation to daily values; (b) 30 runs in which the daily-mean colour index varied randomly in the same range.

to believe that it will eventually be possible to design experiments at sea that can discriminate between the competing parametrizations used in models of the seasonal boundary layer. However, the practical problems are immense and preliminary attempts (e.g. Osborn 1980; Gregg *et al.* 1985), while encouraging, have not achieved the status of a critical test. One of the most serious difficulties to be overcome is the intermittency in the turbulence, which does not feature in the parametrizations, but which poses a severe sampling problem in experiments at sea. The most promising way to overcome that problem is to test the parametrizations by comparing the predicted and observed depth of the turbocline at the base of the mixed layer. Turbocline depth is clearly predicted by all models that incorporate the Richardson number criterion for reverse transition, which is soundly based on theory (Ellison 1957), laboratory experiments (Turner 1973) and field observations (Woods 1969). Significantly different turbocline depths are diagnosed by the different parametrizations. It is attractive as the criterion to be used in experimental tests because the mean turbulent dissipation rate changes by a factor of order one thousand across the turbocline (mW/m^3 above; $\mu W/m^3$ below). That contrast is well above the measurement threshold of turbulence instruments and is so large that the natural intermittency in the turbulence will not lead to serious error in estimating turbocline depth, even in single profiles. We are constructing apparatus to map turbocline depth in the open ocean, but it will be some years before we shall have experimental data suitable for testing boundary layer models in this way. Meanwhile we can determine how the turbocline depth varies in response to changes of surface fluxes according to the various parametrizations. This paper does so for the Kraus–Turner method: readers are invited to repeat our studies with higher-order closure parametrizations.

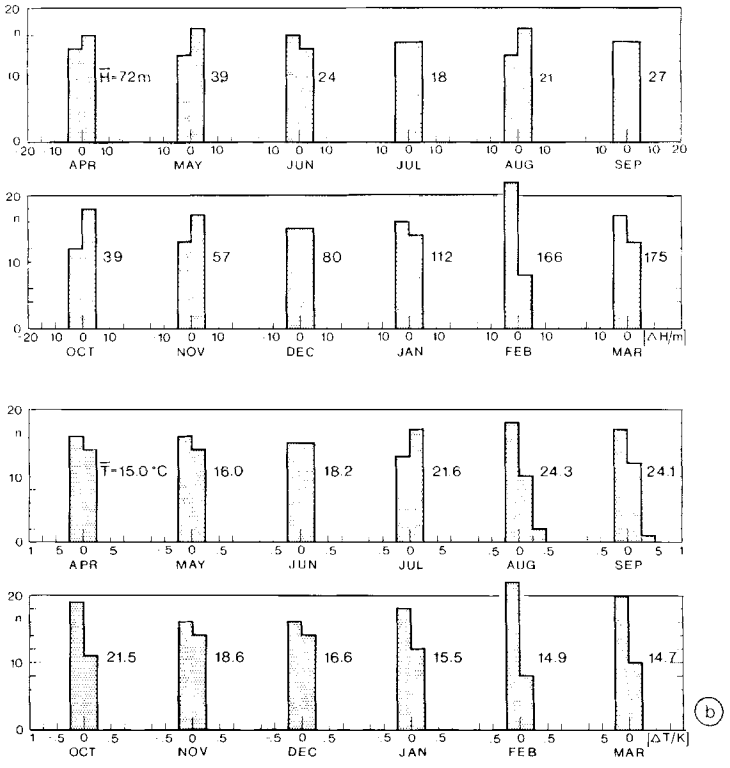

Figure 16 (*continued*).

6. Conclusion

Every day solar heating weakens convection in the mixed layer of the ocean and, for most of the year, quenches it completely for several hours about noon. The consequences of this process for upper ocean mixing, temperature and salinity have been investigated by Eulerian integrations of a one-dimensional model incorporating Kraus–Turner diagnosis of the turbocline depth and forced by astronomical variation of solar elevation plus Bunker's monthly-mean cloud cover and surface meteorology, interpolated spatially to $1°\times1°$ and temporally to one day. A site was chosen (41°N 27°W) where the geostrophic flow is weak and the surface heat budget nearly balances, in order to minimize errors arising from advection, which was not included. Despite these limitations, it is believed that the results may provide insight into the response of the upper ocean to solar heating everywhere. The results lead to a prediction—the diurnal cycle of turbocline depth—that can serve as the target for future experimental tests of that claim.

We investigated the errors arising from integration time steps longer than one hour. If no compensating change is made to the model they give a mixed layer that is deeper and colder than that predicted with one-hour time steps. The error in sea surface temperature is about 30% (10%) of the annual range for time steps of 24 h (12 h). The error in summer mixed layer depth is about 30% (10%) of the value calculated with one-hour time steps. Larger errors in winter mixed layer are due to a phase lag in the seasonal cycle. The error in the vernal correlation of mixed layer depth and temperature leads to significant change in the source term for isopycnic potential vorticity in the seasonal thermocline and will therefore lead to errors in models of gyre circulation based on thermocline ventilation from the seasonal boundary layer. A new parametrization, based on tuning the daily equivalent solar elevation to produce the annual maximum surface temperature calculated with one-hour time steps, greatly reduces these errors.

Using this parametrization with a 12 h time step which captures the essence of day–night response to solar heating, we then explored the sensitivity of the model to changes in the principal variables used in calculating solar heating of the ocean, namely cloud cover and seawater turbidity, with the following conclusions:

(1) The seasonal cycle of the surface buoyancy flux is twice as important as the seasonal cycle of wind stress.
(2) The surface temperature rise for a steady $10\,W/m^2$ increase in solar heating peaks at 1·5 K in September.
(3) The sensitivity of surface temperature anomaly to solar energy anomaly accumulated since the start of the heating season peaks at 0·13 K per W/m^2.
(4) The descent of the turbocline in winter is delayed by four days per W/m^2 for a steady anomaly in solar heating.
(5) Random errors in monthly-mean solar energy lead to random errors of up to ±0·5 K in surface temperature; random errors of ±5 m in turbocline depth.
(6) Daily random errors of cloud cover in the range $(2C_B - 10)$ to 10, where C_B is the climatology mean value (in tenths) interpolated from Bunker's data, lead to bias of up to 0·14 K per W/m^2 and random errors of up to ±1 K in mixed layer temperature; random errors exceeding ±10 m in turbocline depth.
(7) Similar errors in surface temperature and turbocline depth are found for monthly or daily uncertainty in seawater turbidity of ±1 Jerlov unit.

To sum up, it is important to ensure that models used to predict seasonal variation of mixed layer depth and temperature either resolve or parametrize the daytime quenching of convection by solar heating. The model predictions are sensitive to changes in the daily, monthly and annual mean rate of solar heating. Errors at the ±1 K and ±10 m

level are generated by changes of a few points in cloud cover, 10 W/m^2 in surface shortwave radiation flux and one Jerlov unit in seawater turbidity. Such changes lie within the range of experimental uncertainty in global data sets used in climate research, and are comparable with interannual and secular changes expected to occur in solar heating of the ocean.

Acknowledgment

Dr H. J. Isemer kindly made available his re-analysis of the Bunker climatological data (Isemer and Hasse 1985).

References

Baumgartner, A. and Reichel, E. 1975 *The world water balance*. Elsevier, Amsterdam

Bunker, A. F. 1976 Computations of surface energy flux and annual air–sea interaction cycles of the North Atlantic Ocean. *Mon. Wea. Rev.*, **104**, 1122–1140

Bunker, A. F. and Worthington, L. V. 1976 Energy exchange charts of the North Atlantic Ocean. *Bull. Amer. Met. Soc.*, **57**, 670–678

Bunker, A. F., Charnock, H. and Goldsmith, R. A. 1982 A note on the heat balance of the Mediterranean and Red Seas. *J. Mar. Res.*, **40**(Suppl), 73–84

Charlock, T. P. 1982 Mid-latitude model analysis of solar radiation, the upper layers of the sea, and seasonal climate. *J. Geophys. Res.*, **87**, 8923–8930

Dalu, G. A. and Purini, R. 1982 The diurnal thermocline due to buoyant convection. *Quart. J. R. Met. Soc.*, **108**, 929–935

Davis, R. E., de Szoeke, R. and Niiler, P. P. 1981 Variability in the upper ocean during MILE. Pt. II: Modelling the mixed layer response. *Deep-Sea Res.*, **28**, 1453–1476

Defant, A. 1936 *Stratification and circulation of the Atlantic Ocean: The Troposphere*. Scientific results of the German Atlantic-Expedition of the Research Vessel *Meteor* 1925–27, **6**(2). (English edition 1981, Amerind Publ. Co. New Delhi)

1961 *Physical Oceanography*, **1**, Pergamon Press, Oxford

Denman, K. L. and Miyake, M. 1973 Upper Layer Modification at Ocean Station Papa: Observations and simulation. *J. Phys. Oceanogr.*, **3**(2), 185–196

Ellison, T. H. 1957 Turbulent transport of heat and momentum from an infinite rough plane. *J. Fluid Mech.*, **2**, 456–466

Gargett, A. E., Sanford, T. B. and Osborn, T. R. 1979 Surface mixing in the Sargasso Sea. *J. Phys. Oceanogr.*, **9**, 1090–1111

Garwood, R. W. 1979 Air–sea interaction and dynamics of the surface mixed layer. *Rev. Geophys. and Space Science*, **17**, 1507–1524

Gaspar, P. 1985 'An oceanic mixed layer model suitable for climatological studies: Results over several years of simulation'. In Y. Toba and H. Mitsuyasu (eds.) *The Ocean Surface*, 509–516. D. Reidel, Dordrecht

Gautier, C. 1984 'Surface radiation budget'. In C. Gautier and M. Fieux (eds.) *Large-Scale Oceanographic Experiments and Satellites*, 185–203. D. Reidel, Dordrecht

Gordon, C. and Bottomley, M. 1985 'The parametrization of the upper ocean mixed layer in coupled ocean–atmosphere models', in *Coupled Ocean–Atmosphere Circulation Models* (Ed J. C. J. Nihoul), Elsevier, Amsterdam, 613–635.

Gregg, M. C., Peters, H., Wesson, J. C., Oakley, N. S. and Shay, T. J. 1985 Intensive measurements of turbulence and shear in the Equatorial undercurrent. *Nature*, **318**, 140–144

Hofmann, K. 1982 'Ein ein-dimensionales numerisches Modell zur Beschreibung der oberen Schichten des Ozeans'. Diploma thesis, University of Kiel

Isemer, H. J. and Hasse, L. 1985 *The Bunker Climate Atlas of the Atlantic Ocean*, **1**, *Observations*. Springer-Verlag, Berlin

Jerlov, N. G. 1976 *Marine Optics*. Elsevier, Amsterdam

Killworth, P. D.	1983	Deep convection in the world ocean. *Rev. of Geophys. and Space Phys.*, **21(1),** 1–26
Kitaigorodskii, S. A.	1960	On the computation of the thickness of the wind-mixing layer in the ocean. *Izv. Acad. Sci. USSR Geophys.*, **3,** 425–431 (English ed., 284–287)
Kitaigorodskii, S. A., Donelan, M. A., Lumley, J. L. and Terry, E. A.	1983	Wave turbulent interactions in the upper ocean. Part II. Statistical characteristics of wave and turbulent components of the random velocity field in the marine surface layer. *J. Phys. Oceanogr.*, **13,** 1988–1999
Kraus, E. B. and Turner, J. S.	1967	A one-dimensional model of the seasonal thermocline. II. The general theory and its consequences. *Tellus*, **19,** 98–105
Mellor, G. L. and Yamada, T.	1982	Development of a turbulence closure model for geophysical fluid problems. *Rev. Geophys. and Space Phys.*, **20,** 851–876
Nihoul, J. C. J.	1985	*Coupled Ocean–Atmosphere Models.* Elsevier, Amsterdam
Niiler, P. P.	1975	Deepening of the wind-mixed layer. *J. Mar. Res.*, **33(3),** 405–421
	1977	'One-dimensional models of the seasonal thermocline'. In: *The Sea*, **6,** 97–115 (Ed. by E. D. Goldberg, I. N. McCave, J. J. O'Brien, J. H. Steele), Wiley-Interscience, New York.
Niiler, P. P. and Kraus, E. B.	1977	'One-dimensional models of the upper ocean'. In *Modelling and prediction of the upper layers of the ocean* (Ed. by E. B. Kraus), Pergamon Press, 143–177
Oakey, N. S. and Elliott, J. A.	1982	Dissipation within the surface mixed layer. *J. Phys. Oceanogr.*, **12(2),** 171–185
Osborn, T.	1980	Estimates of the local rate of vertical diffusion from dissipation measurements. *ibid.*, **10,** 83–89
Paulson, C. A. and Simpson, J. J.	1977	Irradiance measurements in the upper ocean. *ibid.*, **7,** 952–956
Phillips, O. M.	1977a	'Entrainment'. In *Modelling and prediction of the upper layers of the oceans* (Ed. by E. B. Kraus). Pergamon Press, Oxford, 92–101
	1977b	*Dynamics of the upper ocean* (2nd edition). Cambridge University Press
Pirotton, M.	1985	'Simulation eines Tagesgangs der tropischen Deckschicht und Vergleich mit GATE-C-Daten'. Diploma thesis, University of Kiel
Robinson, M. K., Bauer, R. A. and Schroeder, E. H.	1979	*Atlas of North Atlantic–Indian Ocean Mean Temperatures and Mean Salinities of the Surface Layers.* U.S. Naval Oceanographic Office Ref. Pub. 18, Washington D.C.
Sarmiento, J. L.	1983	A simulation of bomb tritium entry into the Atlantic Ocean. *J. Phys. Oceanogr.*, **13,** 1924–1939
Shay, T. J. and Gregg, M. C.	1984	Turbulence in an oceanic convective layer. *Nature* **310,** 282–285 (see also corrigendum *Nature* **311,** 84)
Simpson, J. J. and Dickey, T. D.	1981a	Alternative parameterizations of downward irradiance and their dynamical significance. *J. Phys. Oceanogr.*, **11,** 876–882
	1981b	The relationship between downward irradiance and upper ocean structure. *ibid.*, **11,** 309–323
Tully, J. P. and Giovando, L. F.	1963	'Seasonal temperature structure in the eastern subarctic Pacific Ocean'. In: *Marine Distributions* (Ed. M. J. Dunbar) Univ. of Toronto Press. Roy. Soc. Canada Spec. Publ. No. 5, 10–36
Turner, J. S.	1969	A note on wind-mixing at the seasonal thermocline. *Deep-Sea Res.*, **16**(Suppl.), 297–300
	1973	*Buoyancy Effects in Fluids.* Cambridge Univ. Press
Wells, N. C.	1979	A coupled ocean–atmosphere experiment: The ocean response. *Quart. J. R. Met. Soc.*, **105,** 355–370
WMO	1984	*Scientific Plan for the World Climate Research Programme.* WCRP Publication Series 2
Woods, J. D.	1968	Diurnal behaviour of the summer thermocline off Malta. *D. Hydrogr. Z.*, **21,** 106–108
	1969	On Richardson's number as a criterion for laminar–turbulent–laminar transition in the ocean and atmosphere. *Radio Science*, **4(12),** 1289–1298

Woods, J. D. 1980 Diurnal and seasonal variation of convection in the wind-mixed layer of the ocean. *Quart. J. R. Met. Soc.*, **106,** 379–394

1984 'Air–sea interaction and the upper ocean in global climate'. In *The Global Climate*, 141–187, (Ed. J. Houghton), Cambridge Univ. Press

1985 'The physics of thermocline ventilation' Chapter 34 in J. C. J. Nihoul (ed.) *Coupled Ocean–Atmosphere Models*. Elsevier, Amsterdam, 543–590

Woods, J. D. and Barkmann, W. 1986 A Lagrangian mixed layer model of 18° water formation. *Nature* (in press)

Woods, J. D. and Onken, R. 1982 Diurnal variation and primary production in the ocean—preliminary results of a Lagrangian ensemble model. *J. Plankton Res.*, **4,** 735–756

Woods, J. D. and Strass, V. 1986 The response of the upper ocean to solar heating. II: The wind-driven current. *Quart. J. R. Met. Soc.*, **112,** 29–42

Woods, J. D., Barkmann, W. and Horch, A. 1984 Solar heating of the oceans—diurnal, seasonal and meridional variation. *Quart. J. R. Met. Soc.*, **110,** 633–656

Woods, J. D., Barkmann, W. and Strass, V. 1985 'Mixed layer and Ekman current response to solar heating'. In Y. Toba and H. Mitsuyasu (eds.) *The Ocean Surface*, 487–507. D. Reidel, Dordrecht.